BANGMOD INTERNATIONAL JOURNAL OF MATHEMATICAL & COMPUTATIONAL SCIENCE
Volume. 7 Number. 1 & 2 (2021)
Pages 74–91

BANGMOD INTERNATIONAL JOURNAL OF
MATHEMATICAL& COMPUTATIONAL SCIENCE ISSN: 2408-154X
https://bangmodmcs.wordpress.com/

IONIC TRANSITION OF ELECTROVISCOUS BOUNDARY LAYER FLOW WITH THE ANALYSIS OF MAXWELL AND NERNST-PLANCK EQUATION

Muhammad Bilal[1], **Anwar Saeed**[2,*], **Asif Ullah Hayat**[3], **Wiyada Kumam**[4]
[1] *City University of Science and Information Technology, Peshawar, K.P.K, Pakistan.*
E-mails: bilalchd345@gmail.com
[2] *Center of Excellence in Theoretical and Computational Science (TaCS-CoE), Faculty of Science, King Mongkuts University of Technology Thonburi (KMUTT), 126 Pracha Uthit Rd., Bang Mod, Thung Khru, Bangkok 10140, Thailand.*
E-mails: anwarsaeed769@gmail.com
[3] *Department of Mathematics, Abdul Wali Khan University, Mardan, 23200, Pakistan.*
E-mails: asifhayat767@gmail.com
[4] *Applied Mathematics for Science and Engineering Research Unit (AMSERU), Program in Applied Statistics, Department of Mathematics and Computer Science, Faculty of Science and Technology, Rajamangala University of Technology Thanyaburi, Thanyaburi, Pathumthani 12110, Thailand.*
E-mails: wiyada.kum@rmutt.ac.th

**Corresponding author.*

Received: 10 November 2021 / Accepted: 23 December 2021

Abstract The aim of the present study is to explore a numerical model for an ionic transition of boundary layer electroviscous fluid flow over a spinning disc. For the purpose, the Nernst-Planck, Maxwell and Poisson's equations are coupled and simulated with the Navier Stokes equation for the ionic species conservation. The basic equations of the electroviscous boundary layer flow are diminished to an ordinary dimensionless system of differential equations. The Matlab built-in package bvp5c has been implemented for the numerical outcomes of the transform equations. The outputs are compared to the existing literature, which seemed to be in good agreement with each other, to ensure that the results are accurate. It has been presumed that the action of Debye length coefficient reduces the potential gradient and exposes an excess number of ions to the flow field, which causes an enhancement in the fluid velocity. The consequences of physical constraints on velocity as well as negative and positive charge profiles are drawn and briefly addressed.

MSC: 47H09
Keywords: Maxwell equation; Dielectric constant; bvp5c technique; Anion and cation ions; Surface charge density; Nernst-Planck equations

1. Introduction

An ionic medium is made up of cations and anions, which have opposite charges. High conductivity, tunable viscosity, low volatility, a broad electrochemical window, and low toxicity are some of the differences between the two [1]. Extractions, gas and liquid chromatography, mass spectrometer, capillary electrophoresis, spectroscopy, electrochemistry, and sensors are only a few of the uses for ionic liquids in chemical analyzing a fluid [2]. Endocrine-disrupting chemicals (EDCs) have recently advanced to the point that they are a threat to the global biological environment and humanity. During the last few decades, various methods such as fluid extracting, Soxhlet extraction and microwave-assisted extraction have been linked to invigilating EDC in soil or, on the other hand, residual conditions [3]. In a couple of these methods, unpredictable natural solvents were used as the extractants, and the bulk of these solvents have a high toxic content, posing a threat to biological communities and humanity. Ionic liquids are a comparatively recent group of solvent that are frequently thought to be less harmful than standard solvents and provide a substitute to chemicals. Human cations and anions make up ionic compounds, which are capable of dissolving a wide spectrum of organic and inorganic compounds [4].
At the micrometer size, physical values that are minor or irrelevant at the full scale may become daunting. The viscous and surface forces are accounted for in the cases. The proximity of surfaces, in particular, means that values such as surface tension and electrokinetic impacts have a greater significance [5]. Isolating and extricating natural contaminants from different matrices, for example, can be accomplished by varying the cation & anion or modifying their sequential, to meet the specifications of numerous technologies [6]. Deng et al. [7] explored the possibility of using imidazolium organic solvents as an energy-efficient green substrate for extracting deep dehydrogenation of ionic liquid. Fluid microextraction and solid stage solvent extraction both employ ionic fluids as a medium [8]. Ionic fluids have efficiently emerged as an excellent dissolvable medium for enzymatic reactions and other nutrient activities [9]. The ionic fluids are made up of ions that maintain their fluid form at temperatures below 1000C or even at room temperature. They've been termed "green solvents" due to their unrivaled qualities, which include a low melting and vapor pressure, thermal stability, minimizing the risk, and reduced negative impacts on the environment [10]. The prerequisite will modify the properties of ILs by changing their constituents (cation and anion) [11]. Protein thermal stabilization is based on the appropriate combination of ILs, that they deposited the protein throughout a high temperature. The spinning disc flow has a long history in the world of computing, with many uses. For example, in processers, heat convection affects the temperature of adjacent electronic components, causing a flow near a spinning hard disc. The invention of centrifugal spinners, external compressors, plate hydrometer, and crystalline processes

Published online: 31 December 2021

Published by Center of Excellence in Theoretical and Computational Science (TaCS-CoE)

Please cite this article as: M. Bilal, et al., Onic transition of electroviscous boundary layer flow with the analysis of Maxwell Nernst-Planck equation, Bangmod Int. J. Math. & Comp. Sci., Vol. 7 No. 1 & 2 (2021) 74–91.

employed in machine memory highlighted the importance of turning disc flows in the mechanic's field Polymer ejection, fluid film accumulation, emulsified coating on photographic films, liquefy swirling, and heat rollers are all examples of boundary extending operations in technology and industries. A thin polymer layer on a constantly changing surface creates a nonuniform pace. The rotating disc electrode device is mostly used to scrutinize the reaction kinetics that has a mass propagation impairment [12]. The MHD, iron ferrite and CNTs hybrid nanofluid flow over an infinite gyrating disc, was studied by Tassaddiq et al. [13]. They reported that increasing the disc spinning velocity significantly increased the thermal energy. The Bingham fluid model was used by Mustafa et al.[14] to investigate viscous dissipation and heat transfer for twirling viscoelastic fluid flow over a permeable rotating disc. A faster thermal efficiency can be achieved by using a higher suction effect at the surface of the disc. The mass and heat flux hypotheses in Oldroyd-B fluid flow over an expanding disc were investigated by Hafeez and Khan [15]. It's worth noting that the solutal relaxation time coefficient has a negative effect on the rate of mass distribution. Gul et al. [16] used many instances to model the hybrid nanoliquid flow between disc and cone. From the study, it was concluded that if the surface temperature remained constant, a spinning disc with a fixed cone could achieve the results for different instruments. Fractional evaluations for Darcy flow over a rotating porous disc were recorded by Li et al. [17]. They used the slip conditions at the spinning disk's tip. Shah et al. [18] examined the performance of effectiveness of chemical catalytic reactors and copper selenide with magnetic field by using MATLAB package bvp4c and RK4 Scheme. The heat transference with the natural convection of hybrid nanoliquid flow in a quadrilateral cavity attached with two animated fins is calculated by Sowmya et al.[19] and Xia et al. [20]. Zaydan et al. [21] thoroughly considered the thermostability of a conducting nanofluid with an outside applied magnetic field as well as vertical flow. During their time modeling any technical breakthroughs, the scientists run into extremely nonlinear BVPs that aren't easily dealed by a straightforward computational approach. To solve BVPs, MATLAB provides the solvers bvp4c and bvp5c. In certain cases, the solvers should be used interchangeably. The key distinction between the solvers is that bvp4c uses a fourth-order algorithm, while bvp5c uses a fifth-order formula. The bvp5c is based on the Lobatto IIIa formula. The algebraic equations are solved directly by bvp5c, and the scheme is supplemented with trivial differential equations to account for undefined parameters [22, 23]. Kumar et al.[24] Khan used a Runge-Kutta-based shooting approach to investigate the energy and mass transport behavior of chemical reactive Maxwell & MHD Casson fluids through a stretched sheet with an interior heat source. Nazir et al. [25] used the finite element technique to explore the effect of nanocrystals on the thermal efficiency of a partly ionized non-Newtonion liquid subjected to magnetic field and thermal radiations. Gopal et al. [26] computed the thermophysical parameters of elevated chemical operations and viscous dissipation on ferrofluid with a continually extending porous sheet using the numerical method RK4 and the shooting methodology. Kumaran et al. [27] used the RK premised shooting mechanism to calculate magnetohydrodynamic thermally reacting Maxwell and Casson fluids past a stretched sheet. Zubaidi et al. [28] and Cui et al. [29]computational reported the role of metallic nanomaterials in atomic fluid phase transitions.

We evaluated an incompressible, axially symmetric 3D ionic flow characteristic over a perforated gyrating disc in the present issue The current work intends to establish a numerical simulation for ionic transportation over a revolving disc. For ionic maintenance of species,

the Nernst-Planck, Maxwell and Poisson's equations are related and simulated. Through the resemblance approach, the modelled equations of the electroviscous boundary layer flow are concentrated to a dimensionless system of ODEs. The Matlab built-in package bvp5c has been implemented for the numerical outcomes of the transform equations. In the coming segment, the problem has been expressed, resolved and discoursed.

2. Formulation of the Problem

We assumed an incompressible ionic fluid flow over a porous surface of a rotating disc. The disk is spinning with an angular velocity as revealed in Figure 1. The fluid is assumed to be of an electrolyte nature, while considering fixed density and thickness Hence, in this sense, the cations (+) and anions (-) have parallel valences z =1. It has been considered that the fluid is infinite and expands in the +ive z-direction. The modeled equations of the flow, electric and magnetic field, and ionic transition are supposed to be dimensionless by using speed $\overrightarrow{V}$,length R^* ,time $\frac{R^*}{\overrightarrow{V}}$ thickness of cations and anions n_0 Here, T is the temperature, k is the Boltzmann coefficient and e are the elementary charge. The dimensionless equations are expressed as [30]:

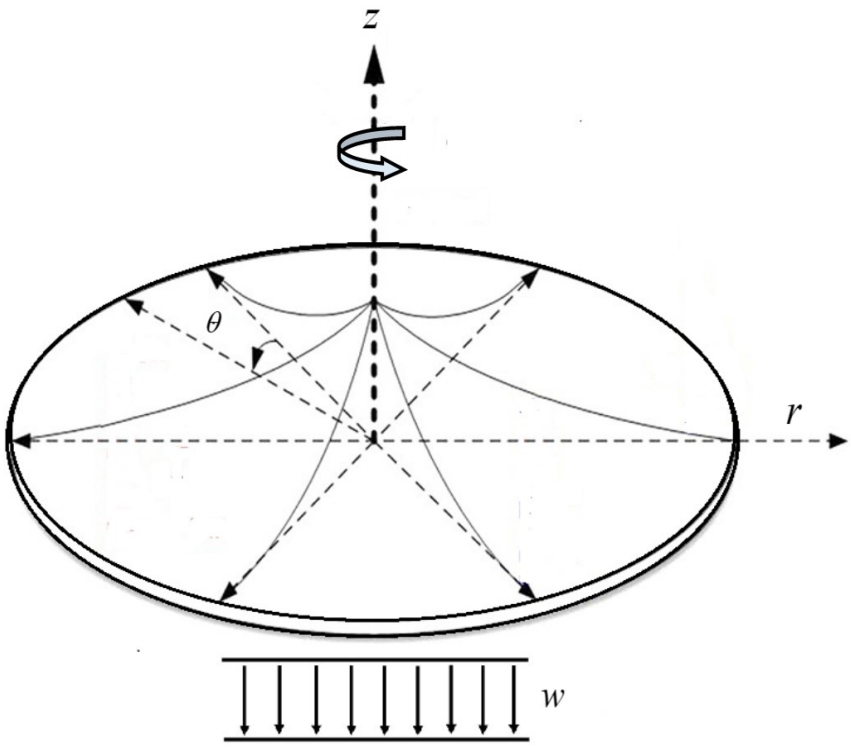

Figure 1. Physical sketch of the spinning cone

$$\nabla.V = 0, \tag{2.1}$$

$$\frac{\partial V}{\partial T} + (V.\nabla)V = -\nabla P + \frac{1}{Re}\nabla.(\nabla V + (\nabla V)^T) - \frac{BK^2}{Re^2}(n_+ - n_-)\nabla U, \tag{2.2}$$

$$\nabla^2.U = -\frac{1}{2}K^2(n_+ - n_-), \tag{2.3}$$

$$\frac{\partial n_+}{\partial t} + \nabla.(Vn_+) = \frac{1}{ReSc}(\nabla^2 n_- + \nabla.(n_+\nabla U)), \tag{2.4}$$

$$\frac{\partial n_-}{\partial t} + \nabla.(Vn_-) = \frac{1}{ReSc}(\nabla^2 n_- + \nabla.(n_+\nabla U)), \tag{2.5}$$

$$\rho\frac{\partial B}{\partial t} = \rho\nabla \times (V \times B) + \frac{\rho}{\sigma\mu_2}\nabla^2 B). \tag{2.6}$$

The dimensionless terms in eq (1-6) are:

$$Re = \frac{\rho\overrightarrow{V}R^*}{\mu_0}, Sc = \frac{\mu_0}{\rho D}, B = \frac{\rho k^2 T^2 \varepsilon_0 \varepsilon}{2Z^2 e^2 (\mu_0)^2}, K^2 = \frac{2Z^2 e^2 n_0 R^{*2}}{\varepsilon_0 \varepsilon k T}, R = \frac{d^2}{V}, R_2 = \frac{\alpha d^2}{2\nu}. \tag{2.7}$$

The parameter K is the inverse Debye length, Sc is the Schmidth number, Re is the Reynold number, B is a fixed constant used for a given at certain temperature respectively. Where, ε_0 and ε is permeability of free space and dielectric constant. R is the rotating Reynolds number, $R_2$is the magnetic based Reynolds number. In which, p_0 and q_0 are the dimensional quantities, which are used to make the B_r and B_z dimensionless.
The boundary conditions for the fluid flow:

$$u = -\frac{\alpha r\gamma}{1-\alpha t}, v = \frac{r\Omega_1}{1-\alpha t}, w = 0, n_+ = n_- = \frac{\alpha}{1-\alpha t}, \nabla.Vn_0 = S \qquad at \;\; Z = 0,$$
$$u \to 0, U \to= 0, v \to= 0, n_+ = n_- \to= 0 \;\; as \;\; z \to \infty \tag{2.8}$$

Equation (1) & (2) are the Navier-Stokes equations with the addition of electrical charge as a body force, due to free charge in the momentum equation. The equation (3) is Poisson relation, which express the electric potential U. The aggregate potential at the uniform disk surface can be rebound as $U = \psi(r) - E\phi(z)$ in which, $\psi(r) = \frac{r^2}{R^2(1-\alpha t)}$ where,E and $\phi(z)$ are the uniform electric field and axial potential energy. Equation (4) & (5) are the Nernst-Plank equations, describing the conservation of particles (n_+, n_-). Equation (6) is the Maxwell equation. Equation (7) displays the boundary conditions, in which $S = \frac{ze\sigma R}{\varepsilon_0 \varepsilon kT}$ is the surface charge density and (n_0) is the external unit vector.

2.1. Similarity Transformation

The following similarity framework has been utilized to modify the system of PDEs to a system of ODEs:

$$u=\frac{\alpha r f^{'}(\eta)}{2(1-\alpha t)},\quad v=\frac{\Omega r g(\eta)}{1-\alpha t},\quad w=\frac{\alpha R f(\eta)}{\sqrt{1-\alpha t}},\quad \eta=\frac{z}{R\sqrt{1-\alpha t}},$$
$$B_r=\frac{\alpha r p_0}{2R(1-\alpha t)}p'(\eta),\quad B_z=\frac{q_0 q(\eta)}{\sqrt{1-\alpha t}},\quad U=-\frac{r^2}{R^2(1-\alpha t)}EH(\eta),$$
$$n_+=\frac{\alpha}{(1-\alpha t)}m'(\eta),\quad n_-=\frac{\alpha}{(1-\alpha t)}n(\eta). \tag{2.9}$$

By implementing equation (9) to equations (1-8), we get:

$$f'''(\eta)=R_2(\frac{\eta}{4}f''(\eta)+\frac{1}{2}f'(\eta)+\frac{1}{4}f'^2(\eta)-(\frac{R}{R_2})^2g^2(\eta)-\frac{1}{2}f(\eta)f''(\eta)$$
$$+2(\frac{R}{R_2})^2g^2(\eta)+\frac{2Bk^2}{\alpha R^2Re^2}, \tag{2.10}$$
$$g''(\eta)=R_2(\frac{\eta}{2}g'(\eta)+g(\eta)+f'(\eta)g(\eta)-f'(\eta)-f(\eta)g'(\eta)), \tag{2.11}$$
$$f^{''}(\eta)=R_2(\frac{\eta}{2}f'(\eta)+\frac{1}{2}f(\eta)-f(\eta)f'(\eta)+\frac{Bk^2E}{\alpha R^2Re^2}(m'(\eta)-n(\eta)h'(\eta))), \tag{2.12}$$
$$m^{''}(\eta)=R^2\alpha ReSc(\frac{\eta}{2}m''(\eta)-m'(\eta)-f(\eta)m''(\eta)+Em''(\eta)h'(\eta)$$
$$+Em'(\eta)h''(\eta)-4m'(\eta)), \tag{2.13}$$
$$n''(\eta)=R^2\alpha ReSc(\frac{\eta}{2}n'(\eta)+n(\eta)-f(\eta)n'(\eta)+4n(\eta)-Eh'(\eta)), \tag{2.14}$$
$$Eh''(\eta)=-\frac{1}{2}k^2R^2(m')(\eta)-n(\eta)-4, \tag{2.15}$$
$$p'''(\eta)=\frac{2R_2}{R}\eta Btp''(\eta)+\frac{4R_2}{R^2}Btp'(\eta)-\frac{2Bt}{R}f'(\eta)h'(\eta)-\frac{2Bt}{R}f''(\eta)h(\eta)$$
$$-\frac{4R_2Bt}{R}f'(\eta)p''(\eta)-\frac{2(R_2)^2Bt}{R}f'(\eta)p'(\eta), \tag{2.16}$$
$$q''=R_2Btq'(\eta)\eta+R_2Btq(\eta)+2R_2Btq(\eta)f'(\eta)+\frac{2(R_2)^2Bt}{R}f(\eta)p'(\eta). \tag{2.17}$$

the modify conditions are

$$f(0)=0,\ f'(0)=-2\gamma,\ g(0)=m(0)=n(0)=1,\ p'(0)=q(0)=1,\ h'(0)=-\frac{RS}{E},$$
$$g(\infty)\to 0,\ f'(\infty)\to 0,\ m(\infty)\to 0\ n(\infty)\to 0,\ p'(\infty)\to 0\ q(\infty)\to 0,\ h'(\infty)\to 0. \tag{2.18}$$

3. Problem Solution

The following variables are introduced in equations (10)-(17) and (18):

$$f = l_1 \ , f' = l_2 \ , f'' = l_3 \ , g = l_4 \ , g' = l_5 \ , m = l_6 \ , m' = l_7 \ , m'' = l_8 \ , n = l_9 \ ,$$
$$n' = l_{10} \ , h = l_{11} \ , h' = l_{12} \ , p = l_{13} \ , p' = l_{14} \ , p'' = l_{15} \ , q = l_{16} \ , q' = l_{17} \ . \tag{3.1}$$

The obtained system of nonlinear 1st order ODEs is:

$$\begin{aligned}
l_1' &= l_2 \ , l_2' = l_3, \\
l_3' &= R_2\Big(\frac{\eta}{2}l_3 + \frac{1}{2}l_2 + \frac{1}{4}l_2^2 - \Big(\frac{R}{R_2}\Big)^2 l_4^2 - \frac{1}{2}l_1 l_3 + 2\Big(\frac{R}{R_2}\Big)l_4^2 + \Big(\frac{2Bk^2}{\alpha R^2 Re^2}\Big)\Big), \\
l_5' &= R_2\Big(\frac{\eta}{2}l_5 + l_4 + l_2 l_4 - l_2 - l_1 l_5\Big), \\
l_8' &= R^2\alpha ReSc\Big(\frac{\eta}{2}l_8 - l_7 - l_1 l_8 + El_8 l_{11} + El_7 l_{12} - 4l_7\Big), \\
l_9' &= R^2\alpha ReSc\Big(\frac{\eta}{2}l_9 + l_8 - l_1 l_9 + 4l_8 - El_4\Big), \\
l_{11}' &= -\frac{1}{2}k^2R^2\Big(l_7 - l_8\Big) - 4, \\
l_{14}' &= \frac{2R_2}{R}\eta Btl_{14} + 4\frac{R_2}{R^2}Btl_{13} - 2\frac{Bt}{R}l_3 l_{11} - 2\frac{Bt}{R}l_3 l_{10} - 4\frac{R_2 Bt}{R}l_2 l_{14} - 2\frac{R_2^2 Bt}{R}l_2 l_{13}.
\end{aligned} \tag{3.2}$$

The boundary conditions are:

$$\begin{aligned}
&l_2(0) = -2\gamma \ , l_4(0) = 1 \ , l_6(0) = l_8(0) = 1 \ , l_{11}I(0) = \frac{-RS}{E} \ , l_{13}(0) = l_{15}(0) = 1 \ , \\
&l_2(\infty) \to 0 \ , l_4(\infty) \to 0 \ , l_6(\infty) = l_8(\infty) \to 0 \ , l_{11}(\infty) \to 0 \ , l_{13}(\infty) = l_{15}(\infty) \to 0 \ .
\end{aligned} \tag{3.3}$$

4. Result and Discussion

4.1. Analysis of result

In the present mathematical model, we have formulated the Nernst-Planck equation, Maxwell equation and Poisson's equations along with the well-known Navier Stokes equation for the ionic fluid transition. The ion-ion interactions have a huge implementation in numerous mathematical models specially in the electro-chemistry. The current mathematical model is a tiny effort towards ionic liquid models, which have a broad range of applications not only in fluid dynamics, but in the fields of electro chemistry as well. For the solution of ionic fluid model, the Matlab built-in package bvp5c is used. Then any other numerical scheme, bvp5c have fast convergence ability.

4.2. Discussion of result

Spinning disk flow of an ionic species has been calculated under the consequences of uniform electric and magnetic field at and ions charged surfaces via Figures (2-7). Figure 1 elaborate an ionic flow mechanism over a spinning disk. Figure 2(a)-(d) revealed the behavior of positive charge profile $m'(\eta)$ against parameter S (surface charge density),

rotational Reynold number R, Reynolds number Re and Schmidth number Sc respectively. It can be perceived that the positive charge profile is reduces with the increment of parameter S.At the disk surface ($\eta = 0$) $+ive$ charge profile remain same, because disk circulate all the charge ions with itself and eventually charge density relics unchanged. We can notice that the formulation of $S = \frac{ze\sigma R}{\varepsilon\varepsilon_0 kT}$ is in inverse relation with $\frac{kT}{ze}$ (electrical potential), which indicates that the positive charge profile decreases as the electric potential drops as shown in Figure 2(a). Increasing Reynolds number leads to a reinforcement of the inertial forces over the frictional viscous forces. The positive charge profile $m'(\eta)$ reduces with the action of rotational Reynold number R, local Reynold number Re, Schmidth number Sc as revealed through Figure 2(c)-(d).

Figure 3(a)-(d) revealed the behavior of negative charge profile$n(\eta)$ against surface charge density S, rotational Reynold number R, Reynolds number Re and Schmidth number Sc respectively. In contrast to positive charge density, negative charge density develops at first, then declines until it approaches zero under the influence of above-mentioned parameters.$S = \frac{ze\sigma R}{\varepsilon\varepsilon_0 kT}$ Here, the rising effect of surface charge density encourage the electric conductivity of the fluid, as a result the negative charge strength reduces, as shown in Figure 3(a). The negative charge profile $n(\eta)$ reduces with the action of rotational Reynold number R, local Reynold number Re, Schmidth number Sc as displayed via Figure 3(c)-(d). The Reynold number Re effect the density of fluid flow, which decreases the negative charge profile as illustrated through Figure 3(b)-(c). Furthermore, the molecular diffusion rate decreases, while kinetic viscosity of fluid enhances with rising effect of Schmidth number, as a result negative charge profile $n(\eta)$ declines Figure 3(d).

Figure 4(a)-(d) illustrated the consequences of several physical entities on radial $f'(\eta)$ velocity. Figure 4(a) elaborate the dominance of parameter S on the velocity distribution. The system is consisting of anion (negative charge) and cation (positive charge) in fluid flow over spinning disc. It has been observed that at less charge density the fluid flows occurred only by the action of electro osmosis. At normal surface density, fluid flow manifest maximum. While, on high charge surface causes the absorption and immobilization of ions near the disc surface. The rising effect of Schmidth number Sc, reduces the thermal diffusivity of fluid flow, which improves the radial velocity profile $f'(\eta)$ as presented in Figure 4(b). Figure 4(c) expressed parameter B impact on velocity profile $f'(\eta)$ as presented in Figure 4(b). Figure 4(c) expressed parameter B impact on velocity profile $f'(\eta)$ B is mostly kept constant for a proposed fluid at a specific temperature. The increment in B reduces the fluid velocity propagation. The behavior of radial velocity profile versus the magnetic Reynolds number is depicted via Figure 4(d). Physically, the positive effect of R_2 , enhances the induction and advection upshot on the fluid flow, which become the cause of reduction in radial velocity profile.

Figure 5(a)-(d) elaborated the nature of axial velocity versus many physical constraints. The same impact of charge density S has been perceived as Fig. 4(a) against axial velocity in Fig. 5(a). The electro-osmosis effect combines with the surface density enhances the axial velocity $f(\eta)$ Figure 5(b) displays the B parameter consequences on the velocity profile. The reverse flow effect has been noticed with an increases of B term. The retarding behavior of velocity versus magnetic force E is communicated in Fig. 5(c). Physically, the magnetic Lorentz forces increase due to the interaction between the electrically conducting fluid and the velocity of the flow which tends to oppose the upward convective motion of the fluid. Consequently, increase the thermal stability of the fluid, that is why, such phenomena have been perceived. Fig. 5(d) is drawn to exhibit the axial

velocity against Debye length coefficient K. Because the potential gradient is not zero near the disk surface, and almost equals to the S. Thats the reason, that an increment K enhances the potential gradient, Because EDLs account up a much smaller fraction of the disc surface and expose more counter-ions to the flow, that improves the axial velocity component.

The influence of parameter S, R_2, E & R are displayed respectively via Fig. 6(a)-(d). Magnetic field strength is always proportional to the surface charge density. The hydration layer is more stable to thermal agitation when the surface charge density is higher. Because the viscous fluid around the ions is polarized to some extent by high charge density, minor ions encounter more resistible forces than bigger ions with lower charge density as observed in Fig. 6(a). Figure 6(b) depicts the reduction in tangential velocity as the magnetic Reynolds number R_2 rises. Physically, increasing the magnetic Reynolds number minimizes the fluid's kinematic viscosity and improves the system's linear dimension, which causes in lowering the fluid's velocity. Figure 6(c) shows how tangential velocity decreases as magnetic strength E grows. The E field provides resistance to the flow profile, causing velocity to drop. Obviously, when the Reynolds number rises, the tangential velocity of the fluid rises, and if the R rises without bounds, the laminar flow will shift to the turbulent flow seen in Figure 6(d).

Figure 7(a)-(d) demonstrated the magnetic strength profile behavior along axial $p'(\eta)$ and radial $q(\eta)$ direction for Batchlor number Bt, rotational Reynold number R, Batchlor number Bt and magnetic Reynold number R_2 respectively. The effect of Batchlor number Bt enhances the axial magnetic strength $p'(\eta)$ profile as illustrated in Fig. (a) & (c). Batchlor number is expressed as $Bt = \sigma\mu_\nu 2$ it measures the fluid slips across the magnetic field. A low current creates a big induced magnetic field when Bt is large. When Bt is weak, however, a moderate-sized current will only create induced fields, which have a minor effect on the applied field. While the Reynold number declines the magnetic strength profile, in both axial and radial magnetic strength profile as shown in Fig. 7(d).

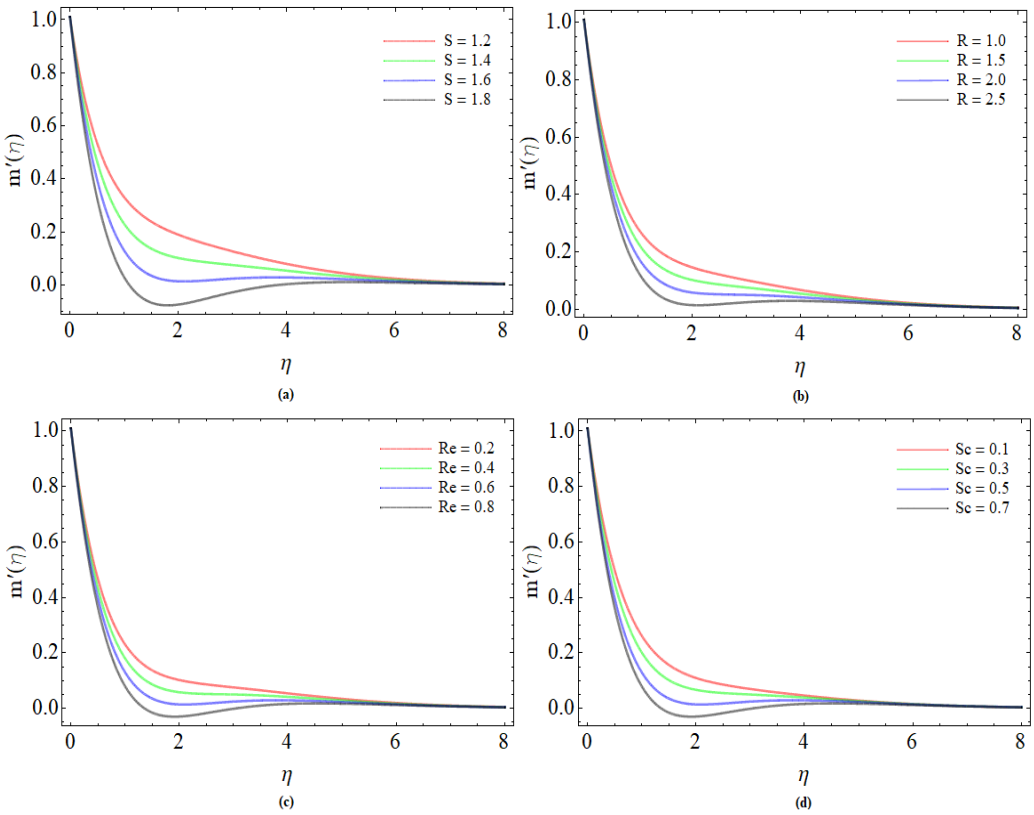

FIGURE 2. Positive charge profile $m'(\eta)$ for (a) surface charge density (b) rotational Reynold number (c) Reynolds number (d) Schmidth number.

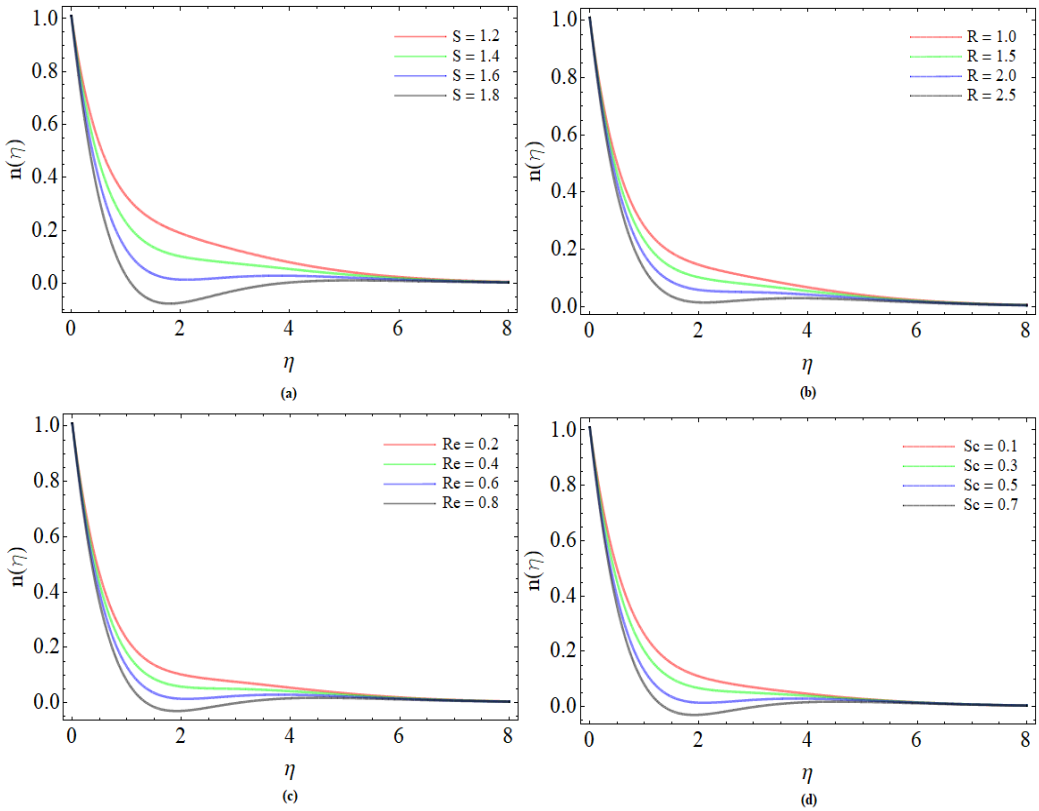

FIGURE 3. Negative charge profile for $n(\eta)$ (a) surface charge density (b) rotational Reynold number (c) Reynolds number (d) Schmidth number.

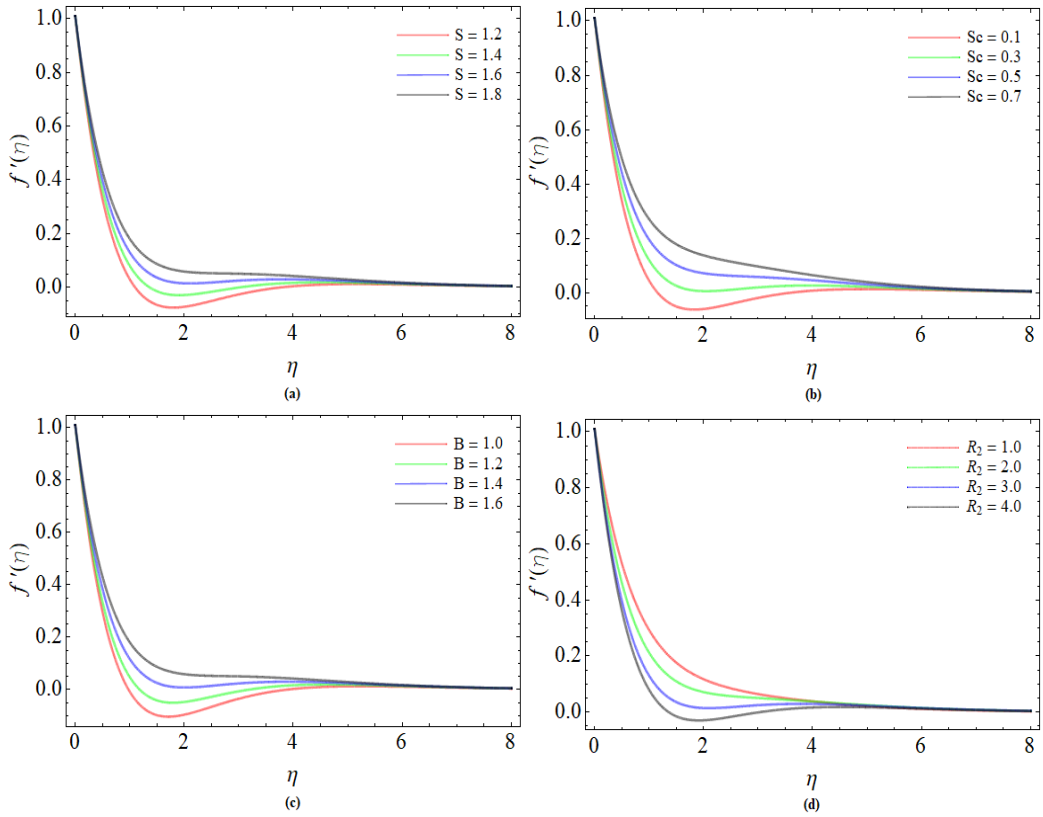

FIGURE 4. Radial velocity profile for $f'(\eta)$ (a) surface charge density (b) Schmidth number (c) Fixed constant (d) magnetic Reynold number.

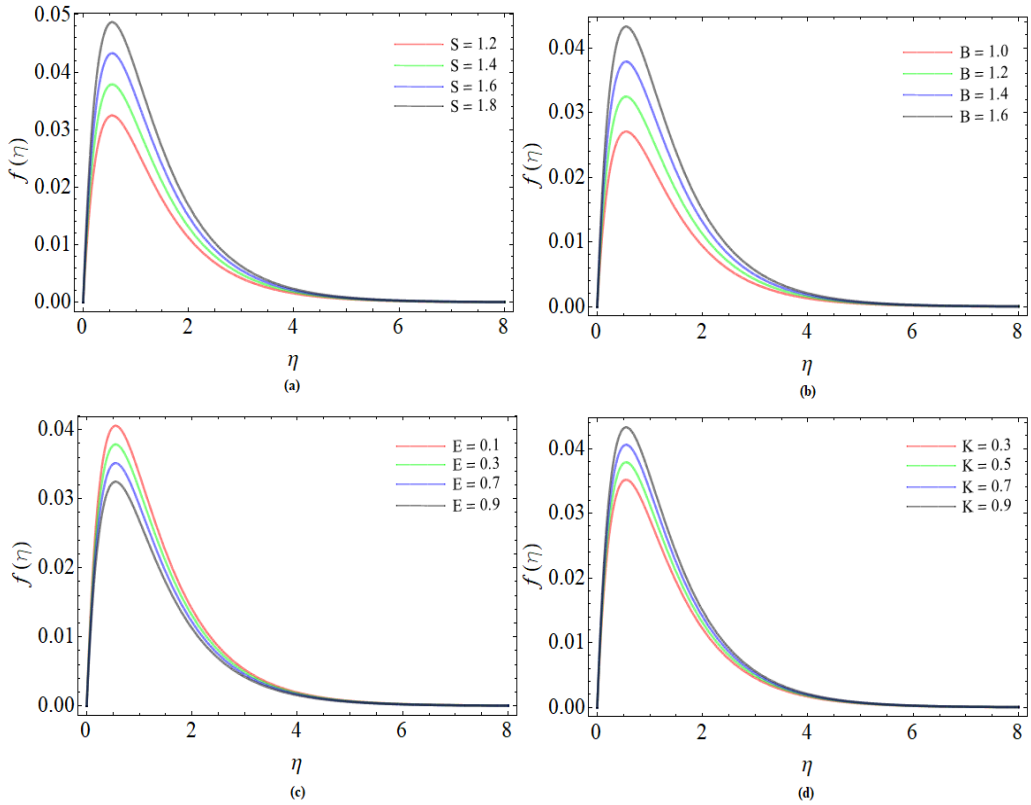

FIGURE 5. Axial velocity profile for $f(\eta)$ (a) surface charge density (b) Fixed constant (c) magnetic strength (d) Debye length.

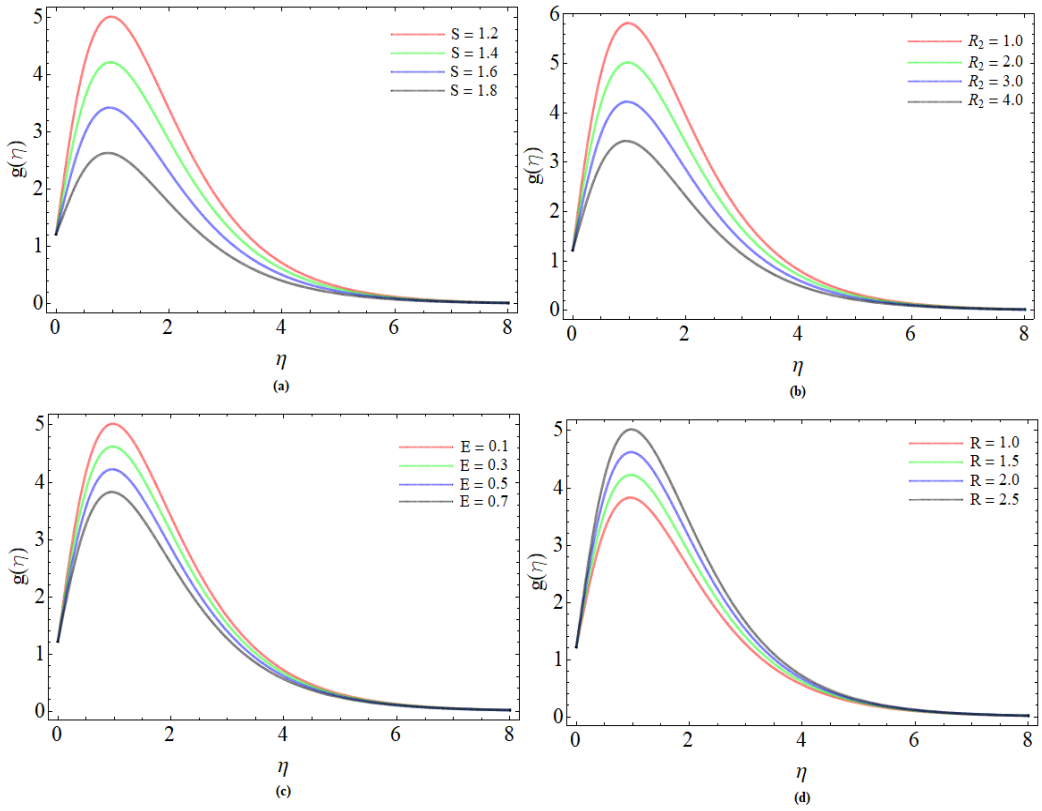

FIGURE 6. Tangential velocity profile for $g(\eta)$ (a) surface charge density (b) magnetic Reynold number (c) magnetic strength (d) Reynold number.

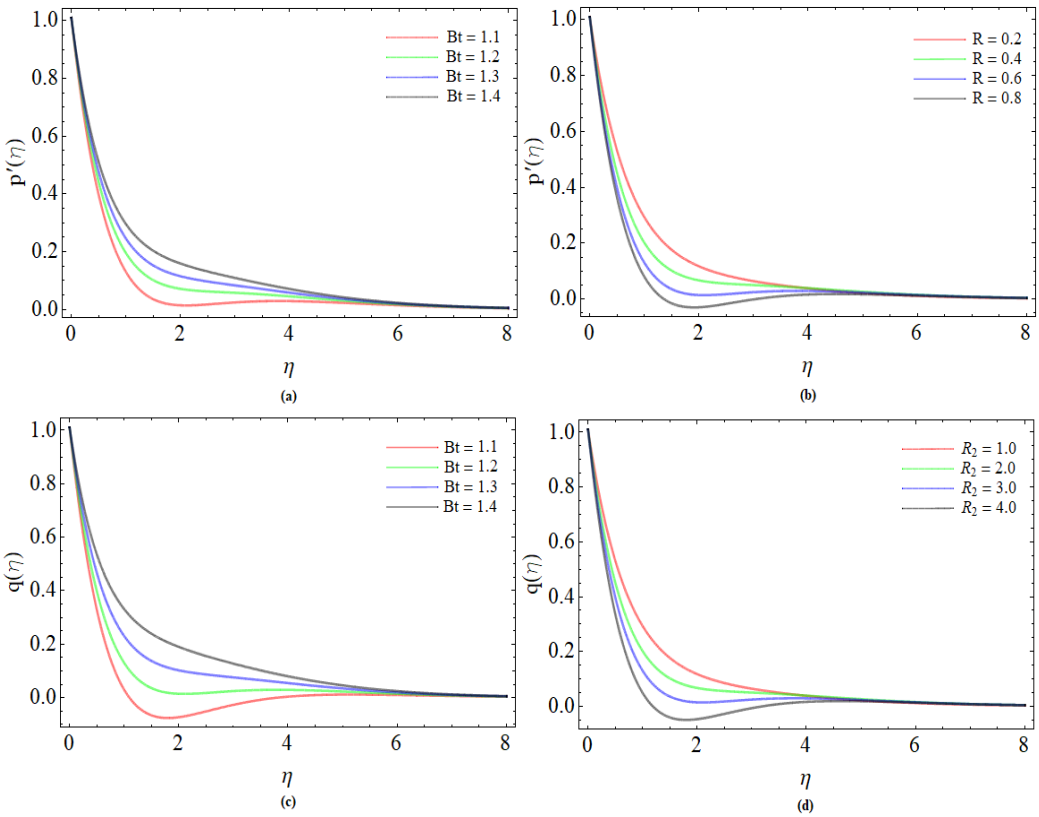

FIGURE 7. The magnetic strength profile behavior along axial $p'(\eta)$ and radial $q(\eta)$ direction for (a) Batchlor number (b) rotational Reynold number (c) Batchlor number (d) magnetic Reynold number.

5. Conclusion

We evaluated an unsteady, axisymmetric $3D$ ionic fluid flow over a permeable spinning disc in the present dilemma. The current effort aspires to establish a numerical analysis for ionic transport in an electroviscous boundary layer flow across a spinning disc. For ionic study the Maxwell equation and Poisson's equation are linked and simulated with the well-known Navier Stokes equations. The following conclusions were reached as a consequence of the aforementioned study and calculation:

- The electrical potential and the surface charge density S are inversely related. As a result, when the electric potential drops, the positive charge per unit volume improves. Work done against an electric field produces electric potential energy.
- The absorption and immobilization of counter ions at the disc surface due to a high charged surface diminishes the radial velocity.
- The Lorentz effect is generated inside the boundary layer by raising the magnetic intensity E, which causes some flow field deceleration, resulting in axial velocity reductions.

- Fluid flows mainly by electro osmotic pressure mechanism at lower charge densities. However, flow is optimum when the surface density is normal.
- The magnetic strength profiles both in axial $p'(\eta)$ and radial$q(\eta)$ direction enhances with the effect of Batchlor number Bt, while the increment in Reynold number declines the magnetic strength profiles.

Competing Interest Statement: No competing interest exists.
Data Availability: The relevant data exist in the article.

References

[1] A. Martinelli, A. Matic, P. Johansson, P. Jacobsson, L. Brjesson, A. Fernicola, H. Ohno, Conformational evolution of TFSI- in protic and aprotic ionic liquids. Journal of Raman Spectroscopy, 42(3)(2011) 522–528.
[2] D. S. Silvester, Recent advances in the use of ionic liquids for electrochemical sensing. Analyst, 136(23)(2011) 4871–4882.
[3] B. Weiss, Endocrine disruptors as a threat to neurological function. Journal of the neurological sciences, 305(1-2)(2011) 11–21.
[4] J. Fan, Y. Fan, Y. Pei, K. Wu, J. Wang, M. Fan, Solvent extraction of selected endocrine-disrupting phenols using ionic liquids. Separation and purification technology, 61(3)(2008) 324–331.
[5] T. M. Squires, S. R. Quake, Microfluidics: Fluid physics at the nanoliter scale. Reviews of modern physics, 77(3)(2005) 977.
[6] M. H. Mallah, F. Shemirani, M. G. Maragheh, Ionic liquids for simultaneous preconcentration of some lanthanoids using dispersive liquid-liquid microextraction technique in uranium dioxide powder. Environmental science & technology, 43(6)(2009) 1947–1951.
[7] N. Deng, M. Li, L. Zhao, C. Lu, S. L. de Rooy, I. M. Warner, Highly efficient extraction of phenolic compounds by use of magnetic room temperature ionic liquids for environmental remediation. Journal of hazardous materials, 192(3)(2011) 1350–1357.
[8] M. Cruz-Vera, R. Lucena, S. Crdenas, M. Valcrcel, Ionic liquid-based dynamic liquid-phase microextraction: Application to the determination of anti-inflammatory drugs in urine samples. Journal of Chromatography A, 1202(1)(2008) 1–7.
[9] B. Dabirmanesh, K. Khajeh, B. Ranjbar, F. Ghazi, A. Heydari, Inhibition mediated stabilization effect of imidazolium based ionic liquids on alcohol dehydrogenase. Journal of Molecular Liquids, 170(2012) 66–71.
[10] C. M. Gordon, New developments in catalysis using ionic liquids. Applied Catalysis A: General, 222(1-2)(2001) 101–117.
[11] M. Freemantle, Photoluminescent films brighten liquid crystal displays. (1998)
[12] W. Chen, M. L. Xu, M. F. Li, Z. Wei, J. Cai, Y. X. Chen, Quantifying intrinsic kinetics of electrochemical reaction controlled by mass transfer of multiple species under rotating disk electrode configuration. Journal of Electroanalytical Chemistry, 872(2020) 114042.
[13] A. Tassaddiq, S. Khan, M. Bilal, T. Gul, S. Mukhtar, Z. Shah, E. Bonyah, Heat and mass transfer together with hybrid nanofluid flow over a rotating disk. AIP Advances, 10(5)(2020) 055317.

[14] M. Mustafa, M. Tabassum, M. Rahi, Second law analysis of heat transfer in swirling flow of Bingham fluid by a rotating disk subjected to suction effect. Thermal Science, 25(1 Part A)(2021) 13–24.
[15] A. Hafeez, M. Khan, Flow of Oldroyd-B fluid caused by a rotating disk featuring the Cattaneo-Christov theory with heat generation/absorption. International Communications in Heat and Mass Transfer, 123(2021) 105179.
[16] T. Gul, M. Bilal, W. Alghamdi, M. I. Asjad, T. Abdeljawad, Hybrid nanofluid flow within the conical gap between the cone and the surface of a rotating disk. Scientific Reports, 11(1)(2021) 1–19.
[17] Y. X. Li, T. Muhammad, M. Bilal, , M. A. Khan, A. Ahmadian, B. A. Pansera, Fractional simulation for Darcy-Forchheimer hybrid nanoliquid flow with partial slip over a spinning disk. Alexandria Engineering Journal, 60(5)(2021) 4787–4796.
[18] N. A. Shah, I. L. Animasaun, J. D. Chung, A. Wakif, F. I. Alao, C. S. K. Raju, Significance of nanoparticles radius, heat flux due to concentration gradient, and mass flux due to temperature gradient: the case of water conveying copper nanoparticles. Scientific Reports, 11(1)(2021) 1–11.
[19] G. Sowmya, B. J. Gireesha, I. L. Animasaun, N. A. Shah, Significance of buoyancy and Lorentz forces on water-conveying iron (III) oxide and silver nanoparticles in a rectangular cavity mounted with two heated fins: heat transfer analysis. Journal of Thermal Analysis and Calorimetry, (2021) 1–16.
[20] W. F. Xia, I. L. Animasaun, A. Wakif, N. A. Shah, S. J. Yook, Gear-generalized differential quadrature analysis of oscillatory convective Taylor-Couette flows of second-grade fluids subject to Lorentz and Darcy-Forchheimer quadratic drag forces. International Communications in Heat and Mass Transfer, 126(2021) 105395.
[21] M. Zaydan, A. Wakif, I. L. Animasaun, U. Khan, D. Baleanu, R. Sehaqui, Significances of blowing and suction processes on the occurrence of thermo-magneto-convection phenomenon in a narrow nanofluidic medium: A revised Buongiorno's nanofluid model. Case Studies in Thermal Engineering, 22(2020) 100726.
[22] L. F. Shampine, J. Kierzenka, M. W. Reichelt, Solving boundary value problems for ordinary differential equations in MATLAB with bvp4c. Tutorial notes, 2000(2000) 1–27.
[23] J. Kierzenka, L. F. Shampine, A BVP solver that controls residual and error. JNAIAM J. Numer. Anal. Ind. Appl. Math, 3(1-2)(2008) 27–41.
[24] M. S. Kumar, N. Sandeep, B. R. Kumar, S. Saleem, A comparative study of chemically reacting 2D flow of Casson and Maxwell fluids. Alexandria Engineering Journal, 57(3)(2018) 2027–2034.
[25] U. Nazir, M. Nawaz, M. M. Alqarni, S. Saleem, Finite element study of flow of partially ionized fluid containing nanoparticles. Arabian Journal for Science and Engineering, 44(12)(2019) 10257–10268.
[26] D. Gopal, S. Saleem, S. Jagadha, F. Ahmad, A. O. Almatroud, N. Kishan, Numerical analysis of higher order chemical reaction on electrically MHD nanofluid under influence of viscous dissipation. Alexandria Engineering Journal, 60(1)(2021) 1861–1871.
[27] G. Kumaran, N. Sandeep, M. E. Ali, Computational analysis of magnetohydrodynamic Casson and Maxwell flows over a stretching sheet with cross diffusion. Results in Physics, 7(2017) 147–155.

[28] A. Al-Zubaidi, M. Nazeer, S. Saleem, F. Hussain, F. Ahmad, Flow of nanofluid towards a Riga surface with heat and mass transfer under the effects of activation energy and thermal radiation. International Journal of Modern Physics B, 35(26)(2021) 2150266.

[29] H. Cui, S. Saleem, J. E. Jam, M. H. Beni, M. Hekmatifar, D. Toghraie, R. Sabetvand, Effects of roughness and radius of nanoparticles on the condensation of nanofluid structures with molecular dynamics simulation: Statistical approach. Journal of the Taiwan Institute of Chemical Engineers, 128(2021) 346–353.

[30] M. Shuaib, R. A. Shah, M. Bilal, Variable thickness flow over a rotating disk under the influence of variable magnetic field: An application to parametric continuation method. Advances in Mechanical Engineering, 12(6)(2020) 1687814020936385.